

## A NEW VECTOR RESONANCE PRODUCTION AT FUTURE COLLIDERS

M. Gintner<sup>1,a,b</sup>, I. Melo<sup>2,a</sup>, B. Trpišová<sup>3,a</sup><sup>a</sup>Physics Dept., University of Žilina, 010 26 Žilina, Slovakia<sup>b</sup>Science and Research Inst., Mathei Bel Univ., 974 01 Banská Bystrica, Slovakia

Received 6 December 2005, in final form 9 May 2006, accepted 10 May 2006

We study the possible production, at future  $e^+e^-$  colliders and at LHC, of a new vector resonance  $\rho$  associated with new strong physics that could be responsible for electroweak symmetry breaking. For the effective description of the vector resonance we introduce a modified Breaking Electroweak Symmetry Strongly model. Since the new resonance exhibits enhanced couplings to the W and Z bosons as well as to the top quark we concentrate on the processes  $e^+e^- \rightarrow t\bar{t}$  and  $e^+e^- \rightarrow \nu_e\bar{\nu}_e t\bar{t}$ . At LHC we study the  $\rho$  production in the process  $pp \rightarrow \rho t\bar{t}$  with  $\rho$  decaying to a  $W^+W^-$  pair. We calculate the cross sections of these processes and of the relevant backgrounds.

PACS: 12.60.Fr, 12.15.Ji

## 1 Introduction

The mechanism of electroweak symmetry breaking (ESB), responsible for the masses of gauge bosons, and perhaps fermions, remains an unsolved mystery. ESB gives rise to the massless Goldstone bosons which, through the Higgs mechanism, become longitudinal components of originally massless  $W^\pm$  and Z bosons. In addition, the mechanism of ESB which is employed in the Standard Model of the electroweak interactions (SM) leads to the presence of the elementary scalar Higgs boson in the particle spectrum. If the coming experiments, an  $e^+e^-$  linear collider (LC) and the Large Hadron Collider (LHC), exclude the existence of the SM Higgs boson, the mechanism for ESB could originate from a strongly interacting new physics which is a scaled-up analogy of the QCD. The other, weakly-coupled, alternative for the mechanism of ESB is represented by supersymmetric theories.

In the absence of the SM Higgs boson, scattering amplitudes of such processes as  $WW \rightarrow WW$  violate a tree-level  $S$ -matrix unitarity at a TeV scale. The unitarity can be restored by new scalar and/or vector particles with enhanced couplings to W, Z bosons and/or to the top quark. Such new particles are predicted by many models. In models of strong ESB (SESB) new composite resonances are expected to appear in analogy with the QCD case.

<sup>1</sup>E-mail address: gintner@fyzika.uct.sk<sup>2</sup>E-mail address: melo@fyzika.uct.sk<sup>3</sup>E-mail address: trpisova@fyzika.uct.sk

A new strong vector resonance in the form of an isospin triplet  $\rho$  ( $\rho^\pm, \rho^0$ ), with mass at 1 TeV scale<sup>4</sup>, is a generic prediction of SESB models. An effective description of  $\rho$  interactions with SM particles was developed and has become known as the BESS (Breaking Electroweak Symmetry Strongly) model [1]. This model is minimal in the sense that  $\rho$  is the only new particle in the spectrum of SM where it replaces the Higgs boson. The BESS model is based on the lowest order effective chiral Lagrangian respecting global  $SU(2)_L \times SU(2)_R$  symmetry which is spontaneously broken down to  $SU(2)_V$  isospin (custodial) symmetry. The symmetry requirements lead to the non-linear sigma model which is then  $SU(2)_L \times U(1)_Y$  gauged. The  $\rho$  resonance is introduced as a  $SU(2)_V$  gauge boson following either Weinberg [2] or hidden symmetry approach [3].

In its original version the BESS model assumes that all fermion generations of the same chirality couple to the  $\rho$  resonance with the same strength [1]. This universality leads to stringent limits on the  $\rho$ -to-fermion couplings from the existing measurements of the SM parameters. In order to relax these limits we introduce some modifications [4] of the BESS model. We break the coupling universality by assuming that only the third generation couples directly, and possibly strongly, to the  $\rho$ -resonance. The symmetries of the model require that the left-handed bottom quark  $b_L$  couples to  $\rho$  with the same strength  $b_1$  as the left-handed top quark  $t_L$ . On the other hand, the  $b_R$  field can be chosen not to interact directly with  $\rho$  at all without affecting the direct  $\rho$ -to- $t_R$  coupling  $b_2$ ; and this is the case in our model. Thus, while the low energy measurements of the  $Zb\bar{b}$  vertex constrain the  $b_1$  coupling to relatively small values [4], they do not limit the direct  $\rho$ -to- $t_R$  coupling  $b_2$ .

The extraordinary value of the top quark mass — far above the masses of other SM fermions and very close to the electroweak scale of 246 GeV — might hint at a special role of the top quark in the mechanism of ESB. This can be taken as a motivation for singling out the  $\rho$  to  $t$ -quark coupling we introduced in our modification of the BESS model.

Processes which depend on the  $\rho$ -to- $t$  coupling can test whether the top quark mass is generated by the same new strong interactions which are responsible for ESB, or by yet additional new strong interactions [5–8]. In the former case, we expect the top quark to couple significantly to the resonances which unitarize  $W_L W_L \rightarrow W_L W_L$  scattering. This could lead to significant event rates in  $W_L W_L \rightarrow t\bar{t}$ . In the latter case, when the mechanism of the top mass generation is different from the  $W$  mass generation, we expect that the top quark does not couple significantly to the new resonances of the strong ESB sector. Then the new resonances observed in the  $W_L W_L \rightarrow W_L W_L$  channel would be suppressed in  $W_L W_L \rightarrow t\bar{t}$ . Many studies have concentrated on the production and signatures of the resonances in  $W_L W_L \rightarrow W_L W_L$  scattering at future lepton and hadron colliders [5].

In our paper we study the potential of several processes to observe the hypothetical vector isovector resonance  $\rho$  introduced within the framework of the modified BESS model. Elsewhere [4], we have studied the corresponding case with a new scalar resonance. The processes considered in this paper will take place either at a future  $e^+e^-$  linear collider, or at the LHC. Here we consider the  $W_L W_L \rightarrow t\bar{t}$  scattering as a subprocess of  $e^+e^- \rightarrow \nu_e \bar{\nu}_e t\bar{t}$  along with the direct production of the vector resonance in  $e^+e^- \rightarrow t\bar{t}$ . The LHC process studied here is  $pp \rightarrow \rho t\bar{t} + X$  with  $\rho$  decaying subsequently to a  $W^+W^-$  pair. Another  $pp$  LHC process which is sensitive to the  $\rho$ -to- $t$  coupling,  $WW \rightarrow \rho \rightarrow t\bar{t}$  fusion, is completely swamped by the huge QCD

---

<sup>4</sup>Throughout the paper we use the units where  $c = \hbar = 1$ .

$\bar{t}\bar{t}$  background [8] and, as we found, so is the resonant process  $q\bar{q} \rightarrow \rho \rightarrow \bar{t}\bar{t}$ .

This paper is organized as follows. In Section 2 we discuss those parts of our  $\rho$  resonance model that describe the direct interactions of the  $\rho$  resonance to quarks of the third generation. In this section the low-energy limits on free parameters of our model as well as the partial wave unitarity limits can be found. In Section 3 we investigate potential of the processes  $e^+e^- \rightarrow \nu_e\bar{\nu}_e\bar{t}\bar{t}$ ,  $e^+e^- \rightarrow \bar{t}\bar{t}$ , and  $pp \rightarrow \rho\bar{t}\bar{t} + X$  to discover the  $\rho$  resonance. These processes are analyzed in Subsections 3.1, 3.2, and 3.3, respectively. Finally, our conclusions can be found in Section 4.

## 2 $\rho$ -resonance model

The most convenient and model-independent approach to the analysis of possible consequences of new strong physics behind ESB is the effective field theory framework. In this approach, an effective Lagrangian has to be built which respects the particle contents and symmetries of the valid low-energy theory, the SM. In the SM the  $SU(2)_L \times SU(2)_R$  global symmetry of the Higgs (ESB) sector is spontaneously broken down to  $SU(2)_V$  isospin symmetry. This symmetry pattern is supported by the relation  $M_W/M_Z = \cos\theta_W$  which is satisfied to high accuracy.

Below the threshold of a new resonance, the ESB sector effective Lagrangian can be built with three pseudoscalar Goldstone bosons. They transform linearly under the  $SU(2)_V$  transformations and nonlinearly under  $SU(2)_L \times SU(2)_R/SU(2)_V$  ones. The requirement of the  $SU(2)_L \times SU(2)_R$  global symmetry leads in the lowest order to the effective Lagrangian known as the non-linear sigma model. From the point of view of the new physics the three Goldstone bosons are analogues of the QCD pions. The non-linear sigma model is made  $SU(2)_L \times U(1)_Y$  locally invariant by the introduction of the massless electroweak gauge bosons. Through the Higgs mechanism the electroweak gauge bosons become massive while the Goldstone bosons transmute to the third components of the gauge bosons.

If there is enough energy to produce a new resonance, its field must be added to the set of building elements of the effective Lagrangian. The  $\rho$  resonance is introduced to the effective Lagrangian as a  $SU(2)_V$  triplet of gauge bosons. The  $\vec{\rho}$  triplet acquires its masses through the Higgs mechanism and mixes with the SM gauge bosons  $\vec{W}$  and  $B$ . In addition, besides the SM interactions of electroweak gauge bosons to fermions, the direct interactions of the  $\rho$  resonance to the third generation of quarks are added. The resulting effective Lagrangian, which is a modified version of the BESS model, is discussed in detail in our previous paper [4].

Here we show only the fermion part of the model which describes the interaction of the  $\rho$ -resonance vector field  $\vec{\rho}_\mu$  with the third generation of quarks  $\psi = (t, b)$

$$\begin{aligned}
L_\rho^f &= ib_1\bar{\psi}_L\xi^\dagger [\not{\partial} - ig''\vec{\rho}\cdot\vec{\tau} + ig'\not{B}/6] \xi\psi_L \\
&+ i b_2\bar{\psi}_R P \xi [\not{\partial} - ig''\vec{\rho}\cdot\vec{\tau} + ig'\not{B}/6] \xi^\dagger P\psi_R \\
&- i \lambda_1\bar{\psi}_L(\xi^\dagger\mathcal{A}\xi)\psi_L + i \lambda_2\bar{\psi}_R P(\xi\mathcal{A}\xi^\dagger)P\psi_R \\
&- (\bar{\psi}_L U^\dagger M\psi_R + \text{h.c.}), \tag{1}
\end{aligned}$$

where  $g''$ ,  $b_{1,2}$ ,  $\lambda_{1,2}$  are free parameters parameterizing new strong physics behind ESB. The Goldstone bosons triplet  $\vec{\pi}$  enters  $L_\rho^f$  through  $\xi = \exp(i\pi_k\tau_k/v)$  and  $U = \xi\xi$ , where  $\tau_k = \sigma_k/2$  stands for the  $SU(2)$  group generators,  $\sigma_k$  denoting the Pauli matrices. Another composite object in  $L_\rho^f$  with well defined transformation properties is  $\mathcal{A}_\mu = \xi^\dagger(D_\mu U)\xi^\dagger/2$  where the covariant

derivative is  $D_\mu U = \partial_\mu U - ig U (\vec{W}_\mu \cdot \vec{\tau}) + ig' (B_\mu \tau_3) U$ . The projection matrix  $P = \text{diag}(1, 0)$  in  $L_\rho^f$  turns off the direct interaction of the  $\rho$  resonance to the right-handed b quark, and the mass matrix  $M = \text{diag}(m_t, m_b)$  contains masses of the third generation of quarks. There is one more free parameter in the BESS Lagrangian, we call it  $a$  [4], which does not occur in  $L_\rho^f$ . The mass  $M_\rho$  of the neutral  $\rho$  resonance depends on  $g''$  and  $a$ ,  $M_\rho = vg''\sqrt{a}/2$ . Thus, in the list of the free parameters of the BESS model,  $a$  can be traded for the mass  $M_\rho$ .

In our modification of the BESS model, the introduction of the  $P$  projection matrix spoils the global isospin  $SU(2)_V$  symmetry of the original sigma model. This is not the only source of the  $SU(2)_V$  symmetry breaking in the model. In this sense the situation is similar to that of the SM. For example, the  $SU(2)_V$  symmetry of the SM Higgs sector is broken by the mass splitting that occurs for the quarks as well as leptons of the same generation.

The relevant parts of our effective chiral Lagrangian [4], of which the most important pieces were shown in Eq. (1), can be cast into a very simple form

$$L = ig_\pi \frac{M_\rho}{v} (\pi^- \partial^\mu \pi^+ - \pi^+ \partial^\mu \pi^-) \tilde{\rho}_\mu^0 + g_V^t \bar{t} \gamma^\mu t \tilde{\rho}_\mu^0 + g_A^t \bar{t} \gamma^\mu \gamma^5 t \tilde{\rho}_\mu^0, \quad (2)$$

where  $\tilde{\rho}_\mu^0$  is the neutral component of the  $\rho$  resonance triplet in the mass eigenstate basis, and  $\pi^\pm = (\pi_1 \mp i\pi_2)/\sqrt{2}$ . The symbol  $v$  denotes the electroweak scale. In Eq. (2) we have introduced the effective coupling constants of the  $\tilde{\rho}\pi^+\pi^-$  and  $\tilde{\rho}t\bar{t}$  vertices. Recall that eventually the  $\pi$  fields play a role of  $W_L$ 's and thus  $g_\pi$  is related to the  $\rho$ -to- $W$  interaction. The relations of  $g_\pi$  and  $g_V^t$  to the free parameters of the Lagrangian  $L_\rho^f$  in (1) are as follows

$$g_\pi = \frac{M_\rho}{2vg''}, \quad (3)$$

$$g_V^t = g'' \frac{b_2}{4(1+b_2)} + \mathcal{O}\left(\frac{g^2}{(g'')^2}\right). \quad (4)$$

We have neglected terms higher in  $g/g''$  assuming  $g'' \gg g$ .

There are six new parameters in our modification of the BESS model:  $g''$ ,  $b_1$ ,  $b_2$ ,  $\lambda_1$ ,  $\lambda_2$ , and  $M_\rho$ . We do not have any experimental constraints on  $M_\rho$ ; the theoretical expectation is around 1–3 TeV. We do have, however, constraints on the parameters  $g''$ ,  $b_1$ ,  $b_2$ , and  $\lambda_1$ ,  $\lambda_2$ . These are due to the corrections that these parameters induce in the SM couplings of the Z and W to fermions at low energies ( $\mathcal{O}(10^2 \text{ GeV})$ ). The low-energy constraints are

$$g'' \gtrsim 10, \quad |b_1 - \lambda_1| \lesssim 0.01, \quad -0.03 \lesssim b_2 - \lambda_2 \lesssim 0.04. \quad (5)$$

In our analysis we assume  $b_1 = \lambda_1 = 0$ . Our results are almost independent of  $\lambda_2$ , leaving  $M_\rho$ ,  $g''$ , and  $b_2$  as free parameters.

If we require the partial wave amplitudes of our model to be unitary up to  $\sqrt{s} = 2.5$  TeV we get the following restrictions on its parameters

$$g_\pi \leq 1.75, \quad g_V^t = g_A^t \leq 1.7, \quad \text{if } M_\rho = 0.7 \text{ TeV}, \quad (6)$$

$$g_\pi \leq 1.50, \quad g_V^t = g_A^t \leq 2.0, \quad \text{if } M_\rho = 1.0 \text{ TeV}. \quad (7)$$

The neutral  $\rho$  resonance at a TeV scale decays predominantly to WW and  $t\bar{t}$ . Thus the total width of the resonance is basically the sum of the widths of these two channels. The  $\rho^0$  width depends on its mass and couplings  $g''$  and  $b_2$ . In Fig. 1 we show the total width of the  $\rho^0$  resonance of the mass of 700 GeV as a function of these two couplings.

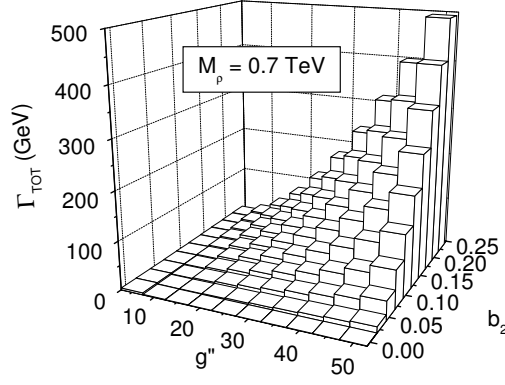


Fig. 1. The total width of the  $\rho^0$  resonance of the mass of 0.7 TeV as a function of the couplings  $g''$  and  $b_2$ .

### 3 Signal and background analysis

#### 3.1 $e^+e^- \rightarrow \nu_e \bar{\nu}_e t \bar{t}$

In our calculations of the signal of the process  $e^+e^- \rightarrow \nu_e \bar{\nu}_e t \bar{t}$  and its backgrounds we used two programs — CompHEP [9] and Pythia [10] into which we had implemented our model. As an example we give the total cross-section  $\sigma$  for the signal process  $e^+e^- \rightarrow \nu_e \bar{\nu}_e t \bar{t}$  with parameters  $M_\rho = 700$  GeV,  $\Gamma_\rho = 12.5$  GeV,  $b_2=0.08$ ,  $g''=20$ , calculated with no cuts for three different energies of collision (CompHEP):

$$\begin{aligned} \sigma &= 0.66 \text{ fb} & \text{at } \sqrt{s} &= 0.8 \text{ TeV}, \\ \sigma &= 1.16 \text{ fb} & \text{at } \sqrt{s} &= 1.0 \text{ TeV}, \\ \sigma &= 3.33 \text{ fb} & \text{at } \sqrt{s} &= 1.5 \text{ TeV}. \end{aligned} \quad (8)$$

We calculated the cross-sections of two major background processes:  $e^+e^- \rightarrow t \bar{t} \gamma$  and  $e^+e^- \rightarrow e^+e^- t \bar{t}$  (Pythia). The irreducible background is represented by the “no-resonance” model (CompHEP) defined as the limit  $M_\rho \rightarrow \infty$ ,  $g'' \rightarrow \infty$ ,  $b_2 = 0$  of our model. This limit effectively removes  $\rho$  from the spectrum and it is identical with the Higgsless SM. The “no-resonance” model is perturbatively unitary up to the scale  $\sqrt{s} \approx m_{WW} \lesssim 1.7$  TeV.

At the energy  $\sqrt{s} = 0.8$  TeV we imposed the following set of cuts

$$\begin{aligned} 500 < m_{t\bar{t}} < 750, & & |\cos \theta_t|, |\cos \theta_{\bar{t}}| < 0.8, \\ 0 < E_t, E_{\bar{t}} < 380, & & 15 < p_T(t\bar{t}) < 300, \\ 20 < p_T(t), p_T(\bar{t}) < 330, & & 50 < m_{miss} < 800, \\ E_{miss} > 90, & & |\cos \theta_{miss}| < 0.96, \end{aligned} \quad (9)$$

where all the values to which it may concern are given in GeV. Following the cuts the total background was reduced from 301.6 fb to 0.13 fb and the signal decreased from 0.66 fb down to

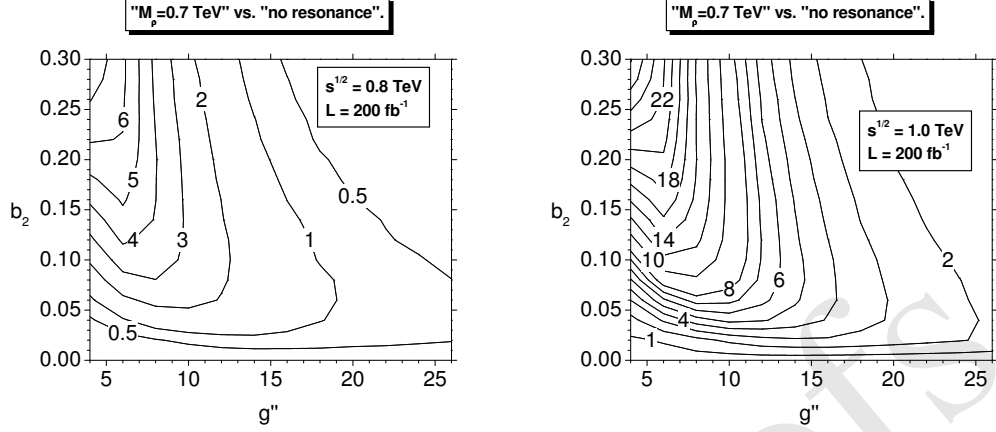


Fig. 2. Sensitivity contours (see Eq. (11)) in the  $(g'', b_2)$  parametric space at the energy of 0.8 and 1 TeV and the integrated luminosity of  $200 \text{ fb}^{-1}$ . The mass of the  $\rho$ -resonance is 0.7 TeV. The cuts (9) and (10) were used, respectively, except that the  $m_{t\bar{t}}$  cut in both cases was changed to  $670 < m_{t\bar{t}} < 730 \text{ GeV}$ . The values of  $R$  are shown on the contours.

0.2 fb. For the collision energy  $\sqrt{s} = 1 \text{ TeV}$  we set

$$\begin{aligned}
 500 < m_{t\bar{t}} < 900, & \quad |\cos \theta_t|, |\cos \theta_{\bar{t}}| < 0.8, \\
 0 < E_t, E_{\bar{t}} < 480, & \quad 15 < p_T(tt) < 400, \\
 20 < p_T(t), p_T(\bar{t}) < 400, & \quad 150 < m_{miss} < 1000, \\
 E_{miss} > 100, & \quad |\cos \theta_{miss}| < 0.96,
 \end{aligned} \tag{10}$$

where all the values to which it may concern are given in GeV. Following the cuts the total background was reduced from 207.3 fb to 0.035 fb while the signal dropped from 1.16 fb down to 0.16 fb. Note that the variable  $\theta_{miss}$  in (9) and (10) stands for the missing momentum angle.

The statistical sensitivity of the process to distinguish between the model with the vector resonance and the “no-resonance” model (reducible backgrounds included) is given by the following relation

$$R = \frac{|N(\rho) - N(\text{no-resonance})|}{\sqrt{N(tt\gamma + e^+e^-tt) + N(\text{no-resonance})}}, \tag{11}$$

where  $N$  denotes the number of events. In Fig. 2 we show  $R$  contours in the  $(g'', b_2)$  parametric space at the energy of 0.8 TeV and 1 TeV and the integrated luminosity of  $200 \text{ fb}^{-1}$ . Cuts (9) and (10) were imposed, respectively, with the exception of the  $m_{t\bar{t}}$  cut that was taken for both energies  $670 < m_{t\bar{t}} < 730 \text{ GeV}$ . We should note, however, that to have a more realistic measure of the statistical significance of the process we would have to extend our analysis further, *i.e.* we should include reconstruction efficiencies and detector effects.

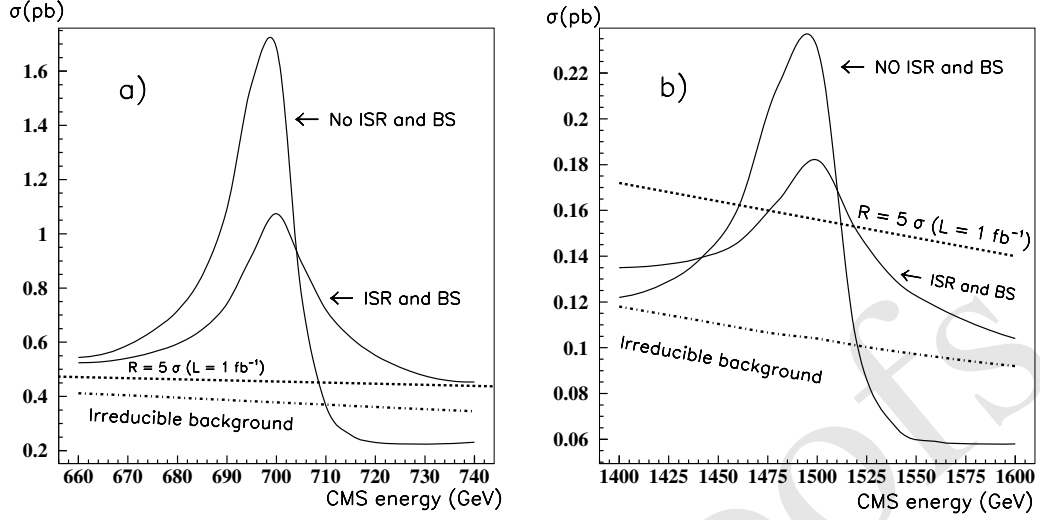


Fig. 3. **a)** The solid curves show the total cross-section of  $e^+e^- \rightarrow t\bar{t}$  as a function of CMS energy without and with initial state radiation (ISR) and beamstrahlung (BS) corrections for a resonance with  $b_2 = 0.08$ ,  $g'' = 20$ ,  $\Gamma = 12.5$  GeV. The dash-dotted straight line represents irreducible (continuum) background with ISR & BS. The dashed line shows the boundary at which the statistical significance  $R = 5$  (Eq. 12) assuming the scanning luminosity  $L_{scan} = 1 \text{ fb}^{-1}$ . The  $\rho$  mass  $M_\rho = 700$  GeV. **b)** Same as a), except that  $M_\rho = 1500$  GeV and the width of the  $\rho$  resonance is changed accordingly to 40.9 GeV.

### 3.2 $e^+e^- \rightarrow t\bar{t}$

The process  $e^+e^- \rightarrow t\bar{t}$  shows surprisingly good sensitivity to the presence of the  $\rho$  resonance. Recall that there is no direct coupling of the  $\rho$  resonance to electrons in the model. Electrons couple to the  $\rho$  resonance only through  $\rho$  mixing with photon and Z-boson. Thus we expect  $\rho$  to couple strongly to the top quark and not to the electron. However, it turns out that the latter coupling is large enough to generate clear peak rising above continuum background.

In Fig. 3 we show the total cross-sections of  $e^+e^- \rightarrow t\bar{t}$  in the region around the peaks of the vector resonances with masses a)  $M_\rho = 0.7$  TeV, and b)  $M_\rho = 1.5$  TeV. For the two masses we obtain two different widths of the  $\rho$  resonance,  $\Gamma_\rho = 12.5$  and 40.9 GeV, respectively, both widths corresponding to the same couple of parameters:  $b_2 = 0.08$ ,  $g'' = 20$ . There are plots of the cross-sections without and with the effects of initial state radiation (ISR) and beamstrahlung (BS) taken into account. The irreducible background represented by the “no-resonance” model cross-section is also shown. All the calculations were performed (CompHEP) without cuts.

The statistical significance  $R$  of the signal is defined as follows

$$R = \frac{|N(\rho) - N(\text{no-resonance})|}{\sqrt{N(\text{no-resonance})}}, \quad (12)$$

where  $N$  denotes the number of events for the model specified in the brackets. In Fig. 3 we also indicate the  $R = 5$  deviation from the no-resonance model assuming the scanning luminosity of



Fig. 4. **(a)** One of 8 Feynman subdiagrams of the dominant gluon-gluon channel contributing to the process  $pp \rightarrow \rho t\bar{t} + X$ . **(b)** One of the subdiagrams that comes from the full calculation of the cross section of  $pp \rightarrow W^+W^-t\bar{t} + X$ .

$1 \text{ fb}^{-1}$  at each  $\sqrt{s}$  step. Our results suggest that under these circumstances, if the relevant  $\sqrt{s}$  region is scanned taking appropriate steps, it should be possible to discover all the cases of the  $\rho$  resonance studied above.

### 3.3 $pp \rightarrow W^+W^-t\bar{t} + X$

We used two approaches in our analysis of the  $pp \rightarrow W^+W^-t\bar{t} + X$  process. In the first one we simplified the problem and treated the process in two steps: we first produced  $\rho$  on-shell as  $pp \rightarrow \rho t\bar{t} + X$  and then included  $\rho \rightarrow W^+W^-$  decay. The cross sections for  $pp \rightarrow W^+W^-t\bar{t} + X$  were found from the cross sections for  $pp \rightarrow \rho t\bar{t} + X$ , multiplied by the corresponding branching ratio for  $\rho \rightarrow W^+W^-$ . The dominant gluon-gluon (gg) channel for the process consists of 8 diagrams, one of them is shown in Fig. 4a. All  $q\bar{q}$  channels were neglected. This first approach is the so called branching ratio approximation (BRA). BRA is a good approximation for the *narrow*  $\rho$  only.

In the second approach we went beyond BRA and computed  $pp \rightarrow W^+W^-t\bar{t} + X$  directly, including the off-shell  $\rho$  contributions (full calculation approach). We thus obtained results which are valid also for the *wide*  $\rho$  resonance case. There are 39 diagrams in the dominant gg channel. They include all 8 diagrams from the BRA approach sensitive to the  $\rho$  presence (one of them is shown in Fig. 4b). The remaining 31 diagrams are much less sensitive to the new physics and thus represent the irreducible background in our studies. We evaluate this background as the “no-resonance” cross-section applying the limit  $M_\rho \rightarrow \infty$ ,  $g'' \rightarrow \infty$ ,  $b_2 = 0$  to our model.

All our results were obtained with the CompHEP package into which we had implemented the effective Lagrangian of our model. In the BRA approach we imposed following cuts on the transverse momentum and rapidity of  $t$  and  $\bar{t}$

$$p_T(t), p_T(\bar{t}) > 100 \text{ GeV}, \quad |Y(t)|, |Y(\bar{t})| < 2 \quad (13)$$

The cross section is plotted in Fig. 5 for  $M_\rho = 0.7 \text{ TeV}$  as a function of  $g''$  and  $b_2$  for the CMS collision energy of 14 TeV (LHC).

In the second approach (full calculation) we use the same rapidity and transverse momentum cuts as before. In addition, we apply the cut on the invariant mass of the  $W^+W^-$  pair:  $M_\rho - 3\Gamma_\rho < M_{WW} < M_\rho + 3\Gamma_\rho$ . As an illustration, the cross-section for  $\rho$  with  $M_\rho = 700 \text{ GeV}$ ,  $b_2 = 0.08$ ,  $g'' = 10$  ( $\Gamma_\rho = 3.95 \text{ GeV}$ ) is  $0.96 \text{ fb}$  (the BRA calculation gives  $1.04 \text{ fb}$ ). The

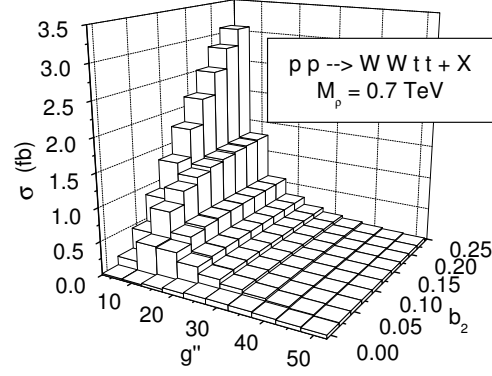


Fig. 5. The BRA cross section of  $pp \rightarrow W^+W^-t\bar{t} + X$  as a function of  $g''$  and  $b_2$ . The  $\rho$  mass is 0.7 TeV and  $\sqrt{s} = 14$  TeV.

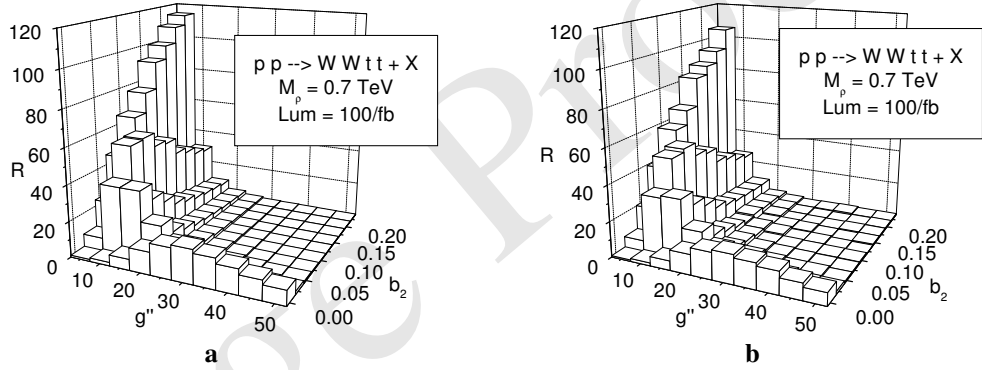


Fig. 6. The statistical significance  $R$  (see Eq. (12)) of  $pp \rightarrow W^+W^-t\bar{t} + X$  as a function of  $g''$  and  $b_2$ . In both graphs the  $\rho$  mass is 0.7 TeV,  $\sqrt{s} = 14$  TeV, and the integrated luminosity is  $100 \text{ fb}^{-1}$ . The plot **a** is based on the BRA calculation, the plot **b** is obtained from the full calculation.

irreducible background cross-section equals to  $\sigma(\text{no-resonance}) = 0.037 \text{ fb}$  in the dominant  $gg$  channel.

The statistical significance  $R$  — as defined by Eq. (12) — is the measure of how well it will be possible to distinguish the  $\rho$  signal from the “no-resonance” signal. We assume the integrated luminosity  $L = 100 \text{ fb}^{-1}$ . The value of  $R$  as a function of  $g''$  and  $b_2$  is plotted in Fig. 6a ( $M_\rho = 0.7 \text{ TeV}$ ) and Fig. 7 ( $M_\rho = 1.5 \text{ TeV}$ ) for the BRA approach and in Fig. 6b ( $M_\rho = 0.7 \text{ TeV}$ ) for the full calculation. While the value of  $R$  in some parts of the  $(g'', b_2)$  parameter space appears to be very promising one has to remember that in this analysis neither the issues of the decays of W boson and top quark, nor the reconstruction efficiencies were taken into account.

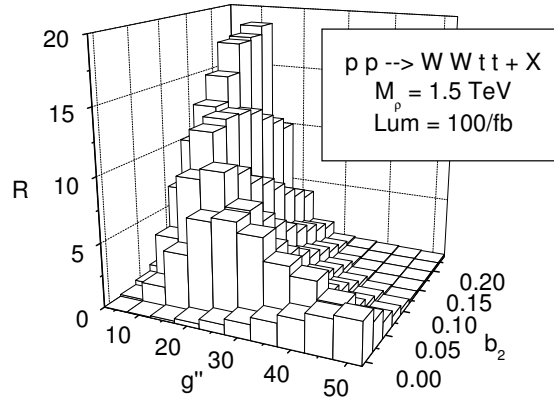


Fig. 7. The statistical significance  $R$  (see Eq. (12)) of  $pp \rightarrow W^+W^-t\bar{t} + X$  as a function of  $g''$  and  $b_2$ . The  $\rho$  mass is 1.5 TeV,  $\sqrt{s} = 14$  TeV, and the integrated luminosity is  $100 \text{ fb}^{-1}$ . The plot is based on the BRA calculation.

#### 4 Conclusions

We have studied a new vector resonance from SESB in the  $e^+e^- \rightarrow \nu\bar{\nu}t\bar{t}$  and  $e^+e^- \rightarrow t\bar{t}$  processes at future  $e^+e^-$  colliders operating at 1 TeV energy scale. We have also studied the resonance in the  $pp \rightarrow W^+W^-t\bar{t} + X$  process at the LHC colliding energy of 14 TeV.

The first process contains  $W_L W_L \rightarrow \rho \rightarrow t\bar{t}$  scattering as its subprocess and is potentially sensitive to the  $\rho t\bar{t}$  coupling  $g_V^t$ . The size of this coupling could hint on the mechanism of the top mass generation. We found (working at the level of undecayed top quarks) that statistical significance  $R$  is as large as 8 for  $M_\rho = 700$  GeV for certain regions of the parameter space allowed by the low energy constraints at a 1 TeV  $e^+e^-$  collider.

While this process is generally sensitive to vector resonances which couple to the top quark and W boson, the second process,  $e^+e^- \rightarrow t\bar{t}$  is sensitive only if the vector resonance coupling to the electron is not negligible. This is exactly the case of our model. In fact, it is the most promising process in this case. To find the resonance peak it is required that the  $e^+e^-$  collider be able to scan the whole energy interval relevant to possible values of  $M_\rho$ . Our results show that applying appropriate scanning step in  $\sqrt{s}$  it should be possible to discover the particular  $\rho$  resonances considered in our analysis if the scanning luminosity is  $1 \text{ fb}^{-1}$  for each value of  $\sqrt{s}$ .

As seen from Fig. 5, the LHC cross sections of  $pp \rightarrow W^+W^-t\bar{t} + X$  are at the level of 1 fb for  $M_\rho = 700$  GeV. The statistical significance  $R$  reaches values as high as 100 (18) for  $M_\rho = 700$  (1500) GeV. The BRA calculations of  $R$  are in good agreement with the full calculation for the narrow  $\rho$  case. We did not consider the issues of the W boson and the top quark decays and reconstruction efficiencies which will significantly modify our predictions of the statistical significance  $R$ . We also did not include reducible background processes. These complex issues require a separate in-depth study. The work on a related process,  $pp \rightarrow t\bar{t}t\bar{t} + X$ , is in progress.

## References

- [1] R. Casalbuoni et al.: *Phys. Lett. B* **155** (1985) 95; D. Dominici: *Riv. Nuovo Cim.* **20** (1997) 1; R. Casalbuoni et al.: *Phys. Lett. B* **258** (1991) 161
- [2] S. Weinberg: *Phys. Rev.* **166** (1968) 1568
- [3] M. Bando, T. Kugo, K. Yamawaki: *Phys. Rep.* **164** (1988) 217
- [4] M. Gintner, I. Melo: *Acta Phys. Slov.* **51** (2001) 139
- [5] T.L.Barklow et al.: *Strong Coupling Electroweak Symmetry Breaking*, Working Group Summary Report from the 1996 DPF/DPB Summer Study New Directions for High Energy Physics, Snowmass, Colorado, June 25 – July 12, 1996, [hep-ph/9704217], and references therein; S.Haywood et al.: *Electroweak Physics*, in *Proceedings of the Workshop on the SM (And More) at the LHC*, CERN 2000-004, Geneva 2000 [hep-ph/0003275]
- [6] E.R.Morales, M.E.Peskin: *Proceedings of the International Workshop on Linear Colliders*, Sitges, Barcelona, Spain, April 28 – May 5, 1999, [hep-ph/9909383]
- [7] S. Godfrey, S-h Zhu: *Phys. Rev. D* **72** (2005) 074011 [hep-ph/0412261]
- [8] T. Han, D. Rainwater, G. Valencia: *Phys. Rev. D* **68** (2003) 015003
- [9] E.Boos et al. [CompHEP Collaboration]: *Nucl. Instrum. Meth. A* **534** (2004) 250 [hep-ph/0403113]; A.Pukhov et al.: [hep-ph/9908288]
- [10] T. Sjostrand et al.: *Computer Physics Commun.* **135** (2001) 238